EAI Endorsed Transactions
on Scalable Information Systems Research Article **EAI.EU**

Adaptive Weighted Kernel Principal Component Analysis and Multi-attribute Decision Making-based Judgment Model for Power Grid Forced Transmission

Qican Dai[1*], Zhiqiang Deng[1], Jianwei Ma[2], Huaiyu Huang[2], Chengjun Wang[3]

[1] Zunyi Power Supply Bureau of Guizhou Power Grid Corporation, Zunyi, Guizhou, 563000
[2] Guizhou Power Grid Power Dispatching and Control Center, Guiyang, Guizhou, 550000
[3]NARI Information & Communication Technology Co., Ltd., Nanjing, Jiangsu, 210000

Abstract

INTRODUCTION: response to the theoretical bottlenecks of the hybrid energy storage system (HESS) when participating in grid regulation.
OBJECTIVES: Such as strong coupling of multi-dimensional state variables, difficulties in coordinating energy storage scheduling with grid stability, and prominent subjectivity in traditional power transfer decisions, a model for AI optimization collaborative control and grid state assessment with HESS as the core control object is proposed.
METHODS: Firstly, based on traditional strong transfer features such as fault characteristics, grid topology, equipment status, and environmental disturbances, the operation state variables of HESS (including state of charge, charging and discharging power, health level, etc.) are introduced to construct a multi-dimensional feature matrix integrating energy storage and the grid, and the objective weighting of each dimension is achieved based on the information entropy theory. Secondly, an adaptive weighted kernel principal component analysis (AW-KPCA) algorithm is proposed, which uses the particle swarm optimization (PSO) algorithm to dynamically adjust the kernel function parameters and feature weights, and incorporates the HESS charging and discharging strategy into the optimization space to achieve joint optimization of energy storage scheduling and high-dimensional feature dimension reduction. The core novelty is the synergistic integration of HESS dynamics into grid feature modeling, PSO-based joint optimization of kernel parameters, feature weights, and storage dispatch, and TOPSIS-driven risk quantification for forced transmission decisions.
RESULTS: Compared with the traditional kernel principal component analysis algorithm, the proposed method improved data processing efficiency by 41.3% and feature extraction accuracy by 15.7%. Finally, the TOPSIS multi-attribute decision-making theory is integrated to build a comprehensive judgment model on the adaptability of forced transportation, quantify the feasibility and risk level of forced transportation, and achieve optimal decision-making under multiple constraints.
CONCLUSION: The simulation test was completed on the IEEE 300-node system and the Guizhou Power Grid Actual Fault Data Set. The accuracy of the proposed model reached 95.7, and its robustness was significantly stronger. The research provides new theoretical and algorithmic support for HESS to participate in the restoration of power grid failures.

Keywords: HESS; Adaptive weighted kernel principal component analysis; Multi-attribute decision-making; TOPSIS method; Particle swarm optimization algorithm

Received on 05 June 2026, accepted on 21 August 2026, published on 08 September 2026

doi: 10.4108/eetsis.13806/ew.13342

*Corresponding author. Email: dqc20260512@163.com

1. Introduction

Power grid forced transmission refers to the operation process in which dispatch operators conduct trial power transmission to faulty lines or equipment based on multi-dimensional information such as fault characteristics, grid topology, equipment status, and environmental disturbances after a power system failure [1-2]. As a key means of power grid fault recovery, the rationality and accuracy of forced transmission operations are directly related to the system power supply recovery speed, safe operation and the overall stability. However, the forced transmission decision is essentially a typical high-dimensional, nonlinear, complex decision-making problem under multi-constraint conditions. Its influencing factors cover multiple dimensions such as fault current amplitude, voltage drop depth, protection action behavior, line importance, circuit breaker health status, meteorological and environmental conditions, etc., and there are complex coupling relationships between various factors. In actual projects, dispatchers often rely on empirical rules to make judgments, which are highly subjective and inefficient in decision-making [3-4]. Therefore, the systematic and objective evaluation of forced transmission feasibility and associated risks—termed "grid forced transmission adaptability judgment"—has become a critical challenge for intelligent power grid fault handling.

At this stage, for power grid forced transmission decision-making, traditional methods mainly rely on power system operating procedures and expert experience to judge forced transmission conditions by setting thresholds or rule libraries. Such methods are highly interpretable, but difficult to cover complex and changeable fault scenarios, and the rule formulation process is highly dependent on manual experience and has poor adaptability [5-6]. Due to the nonlinear and strong coupling relationships between features, traditional feature engineering methods are difficult to effectively extract key discriminant information, resulting in limited model generalization capabilities and difficulty in meeting the interpretability of decision results and controllability of risks in actual dispatch scenarios.

Currently, Alhanaf A S et al. proposed a hybrid deep learning model that combined a 1D Convolutional Neural Network (CNN) and a long-short-term memory network in view of the current situation in the power system where fault detection and location is difficult due to dynamic fault currents and the traditional protection scheme is insufficiently adaptable. The model achieved an average accuracy of more than 99.4% in IEEE 6-node and 9-node tests [7]. The traditional artificial intelligence-based method of the permanent magnet synchronous motor drive system relies many current sampling samples, is susceptible to noise interference, and has high complexity as working conditions change. Therefore, Hang J et al. built a wavelet CNN robust open-circuit fault diagnosis method. This method could diagnose 22 types of faults, and showed excellent noise immunity and robustness in both simulations and experiments [8]. Hajji M et al. proposed a fault detection framework based on machine learning and deep learning in view of the difficult to distinguish between healthy and fault states of grid-connected photovoltaic systems. This method could effectively diagnose different fault types and exhibited high robustness under different irradiation conditions [9]. Kouraichi M et al. reviewed the latest advancements in transmission line fault diagnosis based on deep learning, focusing on key neural network architectures such as convolutional neural networks (CNN), recurrent neural networks (LSTM/GRU), attention mechanisms, and generative models, and discussing challenges such as insufficient data annotation and the detection of rare fault types [10]. Mathebula and Mbuli reviewed the application of TOPSIS multi-attribute decision-making method in the power system, demonstrating its effectiveness in reactive power, power quality, maintenance, and reliability assessment [11]. Meanwhile, Wang et al. systematically reviewed neural network algorithms for battery state-of-energy estimation in smart grid applications [12]. Wang et al. proposed an improved multiple feature-electrochemical thermal coupling model for lithium-ion batteries at low temperatures [13]. A recent study in Energy developed a Bayesian optimization-BiLSTM-UKF fusion algorithm for high-precision battery SOC estimation [14].

Despite these valuable contributions, certain limitations remain in existing approaches. The KPCA-based fault diagnosis methods primarily focus on feature extraction for specific equipment such as transformers, without adapting kernel parameters to the specific characteristics of different fault scenarios. Moreover, existing TOPSIS applications in power systems are mostly confined to equipment state evaluation or operational performance ranking, and have not been extended to forced transmission risk quantification in coordination with energy storage systems. These gaps motivate our work to develop an integrated framework that jointly optimizes feature reduction, HESS dispatch, and risk assessment for forced transmission decisions. Therefore, a method for judging the adaptability of power grid forced transmission is built based on Adaptive Weighted Kernel Principal Component Analysis (AW-KPCA) and multi-attribute decision-making. The Particle Swarm Optimization (PSO) is applied to collaboratively optimize the kernel function parameters and feature weights, and the Technique for Order Preference by Similarity to an Ideal Solution (TOPSIS) multi-attribute decision-making theory is integrated to construct a comprehensive judgment model for forced delivery adaptability. The research aims to achieve efficient dimensionality reduction of high-dimensional redundant features and effective extraction of nonlinear features, while quantifying the feasibility and risk level of forced delivery, so as to achieve optimal decision output under multiple constraints. In summary, the proposed method proceeds in three main steps. First, HESS operating variables are integrated with traditional grid features to construct an extended multi-dimensional feature matrix, with information entropy theory applied for objective weighting. Second, the AW-KPCA algorithm, optimized by PSO, jointly determines kernel parameters, feature weights, and HESS dispatch commands to achieve nonlinear feature reduction while coordinating storage scheduling. Third, the reduced features are fed into the TOPSIS module, which calculates the relative closeness of each forced transmission scheme to the ideal solution and outputs both the optimal dispatch plan and the corresponding risk level. The innovations of this research are as follows: (1) A unified evaluation matrix is constructed by embedding HESS operating variables (SOC, SOH, and power limits) into traditional grid features, allowing energy storage dynamics to be explicitly considered in forced transmission adaptability assessment. (2) An AW-KPCA framework is developed, where PSO jointly optimizes kernel width, feature weights, and HESS dispatch commands within a single fitness function, thus aligning feature reduction with energy storage scheduling. (3) The reduced features are integrated with TOPSIS to output both the optimal storage dispatch plan and the quantified risk level for each scheme, providing dispatchers with a clear and actionable decision basis. These innovations are realized through a unified framework that sequentially performs information entropy-based weighting, PSO-driven joint optimization, and TOPSIS-based risk quantification.

2. Research design

2.1 Forced adaptive multi-dimensional feature matrix construction and adaptive weighting

The influencing factors in judging the power grid's adaptability to forced transmission are complex, the coupling between indicators is strong, and the traditional weighting method is highly subjective. Therefore, the study solves the unreasonable weight distribution in traditional feature construction by establishing a force-feeding adaptive multi-dimensional feature matrix and introducing information entropy theory to adaptively weight each dimensional index. The total number of samples participating in judging the forced transmission adaptability are N, and each sample contains m characteristic indicators, which are derived from the four dimensions of fault characteristics, power grid topology characteristics, equipment status and environmental disturbance. The j-th feature index of the i-th sample is marked x_{ij}. The original multidimensional feature matrix X can be constructed, as shown in formula (1).

$$\mathbf{X}=[x_{ij}]_{N\times m}=\begin{bmatrix} x_{11} & x_{12} & \cdots & x_{1m} \\ x_{21} & x_{22} & \cdots & x_{2m} \\ \vdots & \vdots & \ddots & \vdots \\ x_{N1} & x_{N2} & \cdots & x_{Nm} \end{bmatrix} \quad (1)$$

To ensure comparability between different dimensional indicators, the original feature matrix is standardized. The range standardization method is used to map each indicator to the [0,1] interval, as shown in formula (2).

$$y_{ij}=\frac{x_{ij}-\min_{1\le i\le N} x_{ij}}{\max_{1\le i\le N} x_{ij}-\min_{1\le i\le N} x_{ij}} \quad (2)$$

In formula (2), y_{ij} represents the standardized eigenvalue. To avoid the bias caused by subjective weighting, information entropy theory is introduced to assign objective weights. The rationale is that an indicator with greater dispersion across samples carries more discriminatory information and thus deserves a higher weight, whereas a nearly constant indicator contributes little to classification and should be down-weighted. Information entropy precisely quantifies this dispersion: a smaller entropy value indicates richer information. First, the proportion p_{ij} of the i under the j is given in formula (3).

$$p_{ij}=\frac{y_{ij}}{\sum_{i-1}^{N} y_{ij}}, \quad j=1,2,\cdots,m \quad (3)$$

To avoid the meaningless logarithmic operation when $p_{ij}=0$, the study performs a slight offset on p_{ij}, that is, $p_{ij}=\frac{y_{ij}+\varepsilon}{\sum_{i=1}^{N}(y_{ij}+\varepsilon)}$, where ε represents a very small integer. Secondly, the information entropy e_j of the j is given in formula (4).

$$e_j=-\frac{1}{\ln N}\sum_{i=1}^{N} p_{ij}\ln p_{ij}, \quad j=1,2,\cdots,m \quad (4)$$

From the definition of entropy $0\le e_j\le 1$. When the indicator has completely consistent values in all samples, $e_j=1$ indicates that the indicator does not provide effective information. On the contrary, the greater the dispersion of the indicator, the smaller e_j, and the greater the amount of information. The difference coefficient d_j of the j-th indicator is shown in formula (5).

$$d_j=1-e_j \quad (5)$$

The difference coefficient reflects the effective information amount of the indicator. A large coefficient of difference indicates that the indicator is more important. Accordingly, the objective weight ω_j of the j-th indicator can be expressed based on formula (6).

$$w_j=\frac{d_j}{\sum_{k=1}^{m} d_k}, \quad j=1,2,\cdots,m \quad (6)$$

In formula (6), the weight vector $\omega=[\omega_1,\omega_2,\cdots\omega_m]^T$ satisfies $\sum_{j=1}^{m}\omega_j=1$. Based on the above four traditional dimensions, in order to further integrate the energy storage control capability, a fifth dimension - the operating state variables of the hybrid energy storage system (HESS) is introduced. Each sample contains m_{HESS} related indicators of HESS, and typical variables include: the state of charge (SOC) of the energy storage, the health status (SOH) of the energy storage, the maximum recharge/discharge power, the current recharge/discharge power, the port voltage of the energy storage, the operating temperature, etc. The i-th sample's j-th HESS feature is denoted as $x_{ij}^{(HESS)}$, and together with the features of the original four dimensions, they form an extended multi-dimensional feature matrix. To clarify the origin of the HESS-related variables, these features are generated through a simulation model based on the equivalent circuit model of lithium-ion batteries, combined with predefined operating profiles. Specifically, the SOC of each storage unit is calculated by the ampere-hour integration method, where the instantaneous current is accumulated over time and adjusted by the Coulombic efficiency and rated capacity. The SOH is empirically modeled as a linear decay function of cycle counts and operating temperature, following the degradation model reported in, while the maximum charge/discharge power is constrained by the SOC-dependent power limits recommended by the manufacturer. For the IEEE 300-node system, 20 distributed HESS units are assumed to be connected to selected buses, with rated capacities of 5 MWh, 10 MWh, and 20 MWh. For each fault scenario in both datasets, the HESS operates with a rule-based charge/discharge schedule triggered by voltage deviations and frequency fluctuations. The charging/discharging power commands are updated every 10 seconds over a 5-minute post-fault horizon, generating a total of 30 time-series samples per fault event. Key simulation parameters include: initial SOC range 0.5-0.9, SOC operating limits 0.2-0.95, Coulombic efficiency 0.98, SOH decay rate 0.003% per cycle, and control interval 10 seconds. The subsequent range normalization and information entropy weighting processes cover all m features, ensuring that the HESS state variables obtain objective weights in the dimension reduction and decision-making process. The standardized feature weight matrix is multiplied with the weight vector to obtain a weighted feature matrix. This matrix eliminates the dimensional differences of the original indicators, strengthens the role of high-information indicators in subsequent analysis through information entropy weighting, and provides high-quality input data for the AW-KPCA algorithm [15].

2.2 AW-KPCA design

After constructing and adaptively weighting the forced adaptive multi-dimensional feature matrix, to effectively remove redundant information in high-dimensional features and suppress noise interference, the study further proposes AW-KPCA. This algorithm introduces an adaptive weighting mechanism under the KPCA framework and uses the PSO algorithm to collaboratively optimize kernel parameters and feature weights to achieve efficient dimensionality reduction of high-dimensional nonlinear features [16-17]. The AW-KPCA is illustrated in Figure 1.

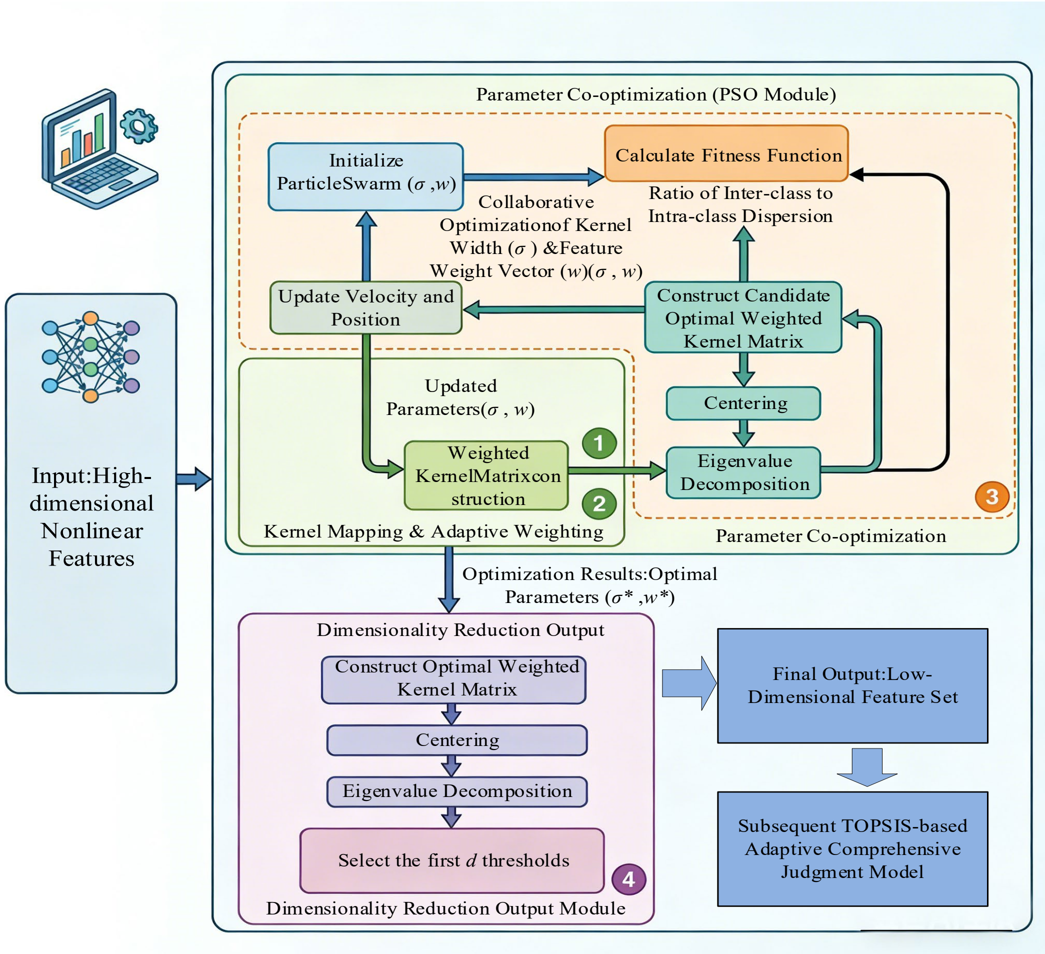

Figure 1. The overall framework of the AW-KPCA

In Figure 1, KPCA maps the original input space to a high-dimensional space through nonlinear mapping and performs linear principal component analysis in this space to extract the nonlinear features of the original data. The input sample set is $Z=[z_1,z_2,\cdots,z_N]^T \in \mathbb{R}^{N\times m}$, where z_i signifies the weighted feature vector of the i. The nonlinear mapping is defined as $\phi:\mathbb{R}^m \to \mathrm{F}$. The input samples are mapped to the high-dimensional feature space F. The mapped samples are recorded as $\phi(z_i)$. In the F, the covariance C is shown in formula (7).

$$C=\frac{1}{N}\sum_{i=1}^{N}\phi(z_i)\phi(z_i)^T \tag{7}$$

The core of KPCA is to solve the eigenvalue problem in the feature space, that is, $Cv=\lambda v$. v represents the eigenvector and λ represents the eigenvalue. Since the explicit form of ϕ is difficult to obtain, KPCA introduces the kernel function technique and defines the kernel matrix $K\in\mathbb{R}^{N\times N}$, whose elements are shown in formula (8).

$$K_{ij}=\langle\phi(z_i),\phi(z_j)\rangle=\kappa(z_i,z_j) \tag{8}$$

In formula (8), κ represents the kernel function, and the study uses the Gaussian radial basis kernel function, as shown in formula (9).

$$\kappa(z_i,z_j)=\exp\left(-\frac{\|z_i-z_j\|^2}{2\sigma^2}\right) \tag{9}$$

In formula (9), σ represents the kernel width parameter, which controls the local scope. The kernel matrix is entered to satisfy the zero-mean condition. The centralized kernel matrix $\tilde{K}$ is given in formula (10).

$$\tilde{K}=K-1_N K-K1_N+1_N K1_N \tag{10}$$

In formula (10), $1_N=\frac{1}{N}1_{N\times N}$. $1_{N\times N}$ is a matrix with all elements $1/N$. Since the traditional KPCA treats all feature indicators as equally important, it fails to reflect the differences among the features. To address this issue, the study introduces a feature weight vector, which scales each feature dimension before calculating the distance. In the weighted Euclidean distance, a larger weight will enhance the contribution of the feature to the overall distance, thereby strengthening its impact on the kernel similarity [18]. For any two samples z_i and z_j, the weighted Euclidean distance is shown in formula (11).

$$d_{\omega}(z_i,z_j)=\sqrt{\sum_{k-1}^{m}\omega_k(z_{ik}-z_{jk})^2} \qquad (11)$$

The weighted distance is substituted into the Gaussian radial basis kernel function to obtain the weighted kernel function, given in formula (12).

$$\kappa_{\omega}(z_i,z_j)=\exp\left(-\frac{d_{\omega}^2(z_i,z_j)}{2\sigma^2}\right) \qquad (12)$$

The weighted kernel matrix K_{ω} is constructed, and the related diagram is shown in Figure 2.

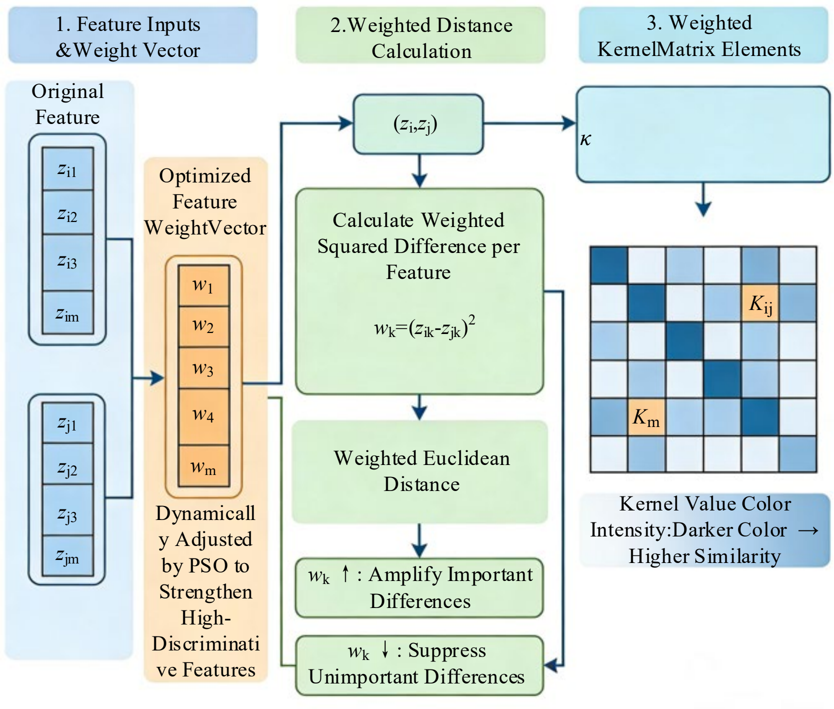

Figure 2. Weighted kernel matrix construction mechanism diagram

In Figure 2, the quality of the weighted kernel matrix is highly dependent on kernel width parameters and feature weight vectors. To obtain the optimal parameter combination, the PSO algorithm is introduced for collaborative optimization. In the fitness function of the PSO algorithm, the separability of features after dimensionality reduction is selected as the optimization goal. The ratio of inter-class dispersion and intra-class dispersion is used as the fitness function, as shown in formula (13).

$$F(\theta)=\frac{\mathrm{tr}(S_b)}{\mathrm{tr}(S_w)} \qquad (13)$$

In formula (13), S_b and S_{ω} signify the inter-class and intra-class scatter matrices. tr represents the trace of the matrix. A larger fitness signifies the stronger discriminative ability of the features after dimensionality reduction in strong adaptive classification. To simultaneously achieve feature dimension reduction, parameter optimization, and energy storage scheduling strategy optimization, the encoding vector of each particle is expanded to formula (14).

$$p=[\varsigma,\omega_1,\omega_2,\ldots,\omega_m,P_{HESS,1},P_{HESS,2},\ldots,P_{HESS,T}] \qquad (14)$$

In formula (14), ς represents the width parameter of the Gaussian kernel, ω represents the feature weight, and P represents the charging and discharging power of HESS.

The corresponding fitness function can be redefined based on formula (15).

$$Fitness=\alpha\cdot\frac{\mathrm{tr}(S_b)}{\mathrm{tr}(S_w)}+\beta\cdot J_{HESS} \qquad (15)$$

In formula (15), J_{HESS} represents the comprehensive revenue indicator for energy storage scheduling, which can include voltage support effect, energy storage lifespan loss cost, energy time-shift revenue, etc. α and β are balance coefficients. Based on this fitness function, PSO simultaneously seeks the optimal feature dimension reduction parameters and the optimal HESS charging and discharging strategy to achieve the joint optimization of energy storage regulation and grid status assessment. Each particle updates its own speed and position based on the individual optimal position p_{best} and the global optimal position g_{best}, as shown in formula (16).

$$v_p^{(t+1)} = \gamma v_p^{(t)} + c_1 r_1 (p_{\text{best}}^{(t)} - \theta_p^{(t)}) + c_2 r_2 (g_{\text{best}}^{(t)} - \theta_p^{(t)}) \theta_p^{(t+1)} = \theta_p^{(t)} + v_p^{(t+1)} \quad (16)$$

In formula (16), γ signifies the inertia weight. c_1 and c_2 signify learning factors, respectively. r_1 and r_2 signify random numbers in the range [0,1], and the weight vector is normalized after each iteration to satisfy the constraint that the sum is 1. The update of particle velocity and position still follows formula (16). The feature weight vector is normalized after each iteration, while ensuring that the HESS power command meets the operational constraints. The collaborative optimization of the PSO algorithm is shown in Figure 3.

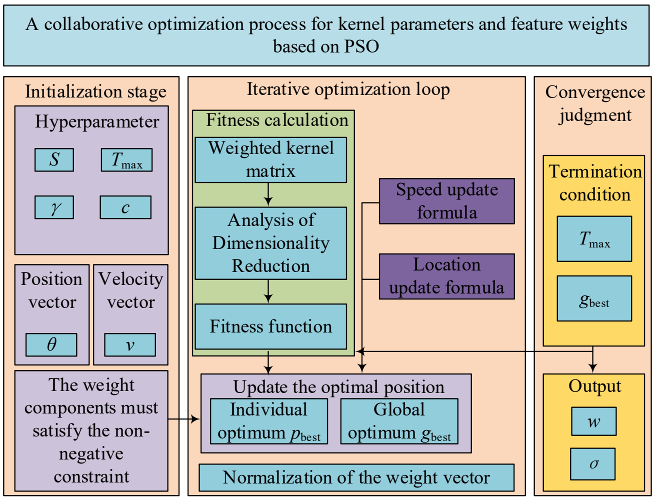

Figure 3. PSO collaborative optimization process

Figure 3 shows the collaborative optimization process of kernel parameters and feature weights based on PSO. Through the collaborative search of particle swarms in the solution space, this process overcomes the shortcomings of traditional methods that rely on artificial experience selection of kernel parameters and weights, adaptively optimizes parameter combinations, and lays the foundation for key parameters for constructing weighted kernel matrices and subsequent efficient dimensionality reduction.

2.3 Construction of a comprehensive judgment model on forced delivery adaptability based on TOPSIS

On the basis of completing the dimensionality reduction of high-dimensional features and extracting low-dimensional discriminant features, to further quantify the feasibility and risk level of the forced delivery scheme, the study further builds a comprehensive judgment model for forced delivery adaptability based on TOPSIS. In the research framework, each "evaluation scheme" to be assessed is actually defined by the "strong sending operation mode (such as attempting to send the line number)" and the "HESS charging and discharging plan (power instructions for each time period)". Therefore, each row of the decision matrix corresponds to a combination of a "strong sending scheme + HESS scheduling scheme". After dimensionality reduction by AW-KPCA, the low-dimensional features in the resulting set implicitly contain the contribution of the HESS state variables, and together with the HESS scheduling performance indicators (such as SOC deviation, power fluctuation suppression rate), they constitute the decision matrix. TOPSIS determines the relative order of alternatives by calculating the closeness of each alternative to the positive ideal solution and the negative ideal solution. It is suitable for multi-index comprehensive evaluation scenarios in power grid forced transmission adaptability. In the forced delivery adaptability evaluation system, after dimensionality reduction by AW-KPCA, the dimensionality reduction feature set $H \in \mathbb{R}^{N \times d}$ is obtained. The decision matrix is constructed by integrating two categories of indicators. The first category comprises the low-dimensional feature set obtained from AW-KPCA, which encodes the intrinsic characteristics of each forced transmission scheme, including fault signatures, topological properties, equipment conditions, environmental disturbances, and HESS operating states. These features reflect the overall grid-storage system condition. The second category comprises operational performance indicators of HESS, including SOC deviation from the desired range, power fluctuation suppression rate, and voltage support effectiveness. These indicators directly measure the regulatory performance of energy storage under each candidate schedule. The classification basis is that feature indicators describe the system state, while operational indicators evaluate the control outcome. All indicators are normalized and weighted before being fed into the TOPSIS evaluation. There are n forced delivery plans to be evaluated, and each plan is represented by d evaluation indicators to construct a decision matrix. To eliminate the dimensional influence and reflect the difference in index importance, the decision matrix is first vector normalized and then multiplied by the feature weight vector to obtain the weighted normalized decision matrix $U=[u_{ij}]_{n\times d}$. The relevant mathematical expression is shown in formula (17).

$$u_{ij}=w_j\cdot\frac{r_{ij}}{\sqrt{\sum_{k-1}^{n}r_{kj}^2}} \tag{17}$$

In formula (17), r_{ij} signifies the original value of the i -th plan on the j -th indicator. When calculating positive and negative ideal solutions and relative closeness, the positive ideal solution A^+ and the negative ideal solution A^- are defined as the optimal and worst values of each indicator in the weighted normalized matrix, respectively. The Euclidean distance between each solution and the A^+ and A^- is calculated. The relative closeness T_i is obtained, as shown in formula (18).

$$T_i=\frac{D_i^-}{D_i^+-D_i^-} \tag{18}$$

In formula (18), D_i^+ and D_i^- signify the Euclidean distances of positive and negative ideal solutions. $T_i\in[0,1]$, and a higher value indicates the better plan, the stronger the adaptability of forced delivery. The final calculation results of the forced delivery plan are presented in Table 1.

Table 1. The result of the proximity of the forced transmission scheme

Scheme Number	Relative proximity	Sort	Risk level
Scheme 1	0.852	1	Low risk
Scheme 2	0.734	2	Low risk
Scheme 3	0.615	3	Medium risk
Scheme 4	0.523	4	Medium risk High risk
Scheme 5	0.387	5	High risk
Scheme 6	0.241	6	High risk

In Table 1, based on the value range of the relative fit degree T_i and combined with the actual situation of the power grid forced transmission project, the forced transmission adaptability has low risk, medium risk, and high risk. Figure 4 presents the risk level division.

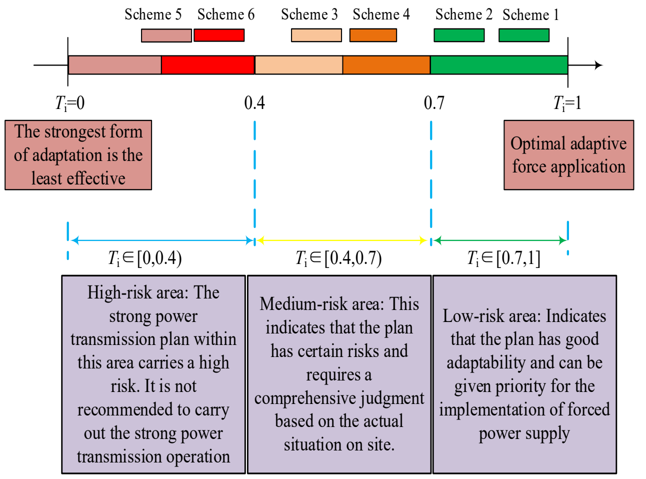

Figure 4. Risk level classification diagram

In Figure 4, the marked points of Plans 1 and 2 fall in the green low-risk zone, Plans 3 and 4 fall in the yellow medium-risk zone, Plans 5 and 6 fall in the red high-risk zone, which visually presents the ranking of each plan, and can provide clear decision-making reference for dispatch operators.

3. Results

3.1 AW-KPCA performance verification

To verify the proposed AW-KPCA in dimensionality reduction of power grid forced transmission adaptability features, simulation experiments were conducted based on the IEEE 300-node system and the Guizhou Power Grid Actual Fault Data Set. Table 2 presents the experimental environment and AW-KPCA parameter settings.

Table 2. Experimental settings

Category	Configuration	Parameter	Value /

			Range
CPU	Intel Core i9-13900K, 24 cores, 3.0 GHz	PSO population size	30
RAM	64 GB DDR5-5600 MHz	PSO maximum iterations	100
GPU	NVIDIA GeForce RTX 4090, 24 GB GDDR6X	Inertia weight	0.7
Operating System	Windows 11 Professional 64-bit	Learning factors	2
Programming Language	Python 3.10	Kernel width σσ	[0.1,10.0]
Core Libraries	NumPy 1.24, SciPy 1.10, Scikit-learn 1.2, Matplotlib 3.7	Feature weights ωjωj	[0,1]
/	/	Cumulative variance contribution rate	≥85%
/	/	Convergence tolerance	10−4

Based on the experimental environment and algorithm parameters in Table 2, the data set is the internationally accepted IEEE 300-node system simulation data set, and the second is the Guizhou Power Grid Actual Fault Data Set. The IEEE 300-node system is a large-scale transmission network standard test system, including 300 bus nodes, 411 transmission lines, and several transformers, generators and other equipment. The fault types include Single-phase Grounding (SG), Two-phase Short Circuit (TSC), Two-phase Grounding Short Circuit (TGS), and Three-phase Short Circuit (TPS). Each sample collection covers 23-dimensional original feature indicators. The Guizhou Power Grid Actual Fault Data Set collects actual fault record data of China's Guizhou Power Grid from 2019 to 2024, with a total of 156 sets of real fault cases. This data set covers transmission line faults at voltage levels of 110kV and above in Guizhou Province. To objectively assess the performance, the two data sets were classified into training, verification and test sin a 7:2:1. The study also selected traditional KPCA, t-Distributed Stochastic Neighbor Embedding (t-SNE) and Stacked Autoencoder (SAE) for controlled experiments. The data processing efficiency of the four algorithms is shown in Figure 5.

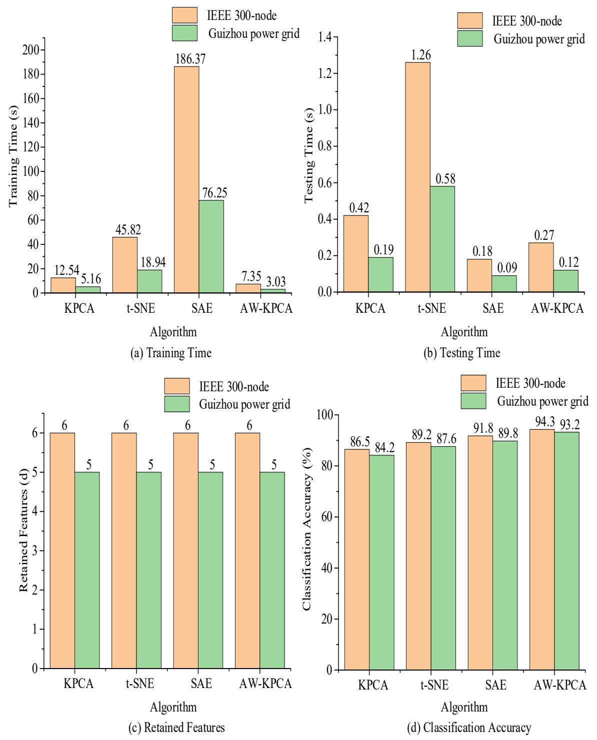

Figure 5. Comparison of data processing efficiency

In Figure 5, on the IEEE 300-node data set, the training time of AW-KPCA was 7.35 seconds, which was 41.3% lower than that of traditional KPCA (12.54 seconds), and the classification accuracy was increased to 94.3%, which was about 7.8%, 5.1% and 2.5% higher than that of KPCA, t-SNE and SAE, respectively. On the Guizhou Power Grid Actual Fault Data Set, AW-KPCA also achieved the best performance, with a training time of 3.03 seconds and a classification accuracy of 93.2%, which was 9.0%, 5.6%, and 3.4% higher than that of KPCA, t-SNE and SAE, respectively. In summary, AW-KPCA has optimized data processing efficiency and classification accuracy on both data sets, verifying its superiority and robustness in data scenarios of different scales and sources. The feature extraction accuracy is compared, as presented in Table 3.

Table 3. Feature extraction accuracy across different dimensionality reduction algorithms

Algorithm	Dataset	Feature Extraction Accuracy (%)	Improvement over KPCA (%)
KPCA	IEEE 300-node	82.4	/
t-SNE		86.3	4.7
SAE		88.9	7.9
AW-KPCA (Proposed)		95.3	15.7
KPCA	Guizhou power grid	80.5	/
t-SNE		84.7	5.2
SAE		87.2	8.3
AW-KPCA (Proposed)		93.6	16.3

In Table 3, on the IEEE 300-node data set, the feature extraction accuracy of AW-KPCA reached 95.3%, which was 15.7% higher than that of traditional KPCA (82.4%) and higher than that of t-SNE (86.3%) and SAE (88.9%). On the Guizhou Power Grid Actual Fault Data Set, AW-KPCA also achieved a feature extraction accuracy of 93.6%, which was 16.3% higher than that of KPCA (80.5%), and better than that of t-SNE (84.7%) and SAE (87.2%) by 8.9% and 6.4%, respectively. In summary, AW-KPCA achieves significantly better feature extraction accuracy than traditional KPCA and other control algorithms on both data sets, proving the effectiveness and advancement in dimensionality reduction of power grid forced transmission adaptability features.

3.2 Simulation results of comprehensive judgment model on forced delivery adaptability

After analyzing the performance of the AW-KPCA, the research further analyzed the simulation results of the forced delivery adaptability comprehensive judgment model. Before presenting the results, it is necessary to clarify the correspondence between the evaluation metrics and the task formulation. The forced transmission adaptability problem is inherently a multi-criteria decision-making task, where each candidate scheme is ranked by its relative closeness to the ideal solution. However, to quantitatively validate the model's discriminative power, we reformulate the top-ranked scheme selection as a classification problem: a scheme is considered correctly judged if its TOPSIS-derived risk level matches the ground-truth risk level determined by domain experts. Under this formulation, accuracy measures the overall proportion of correctly classified schemes, precision and recall evaluate class-wise performance, and F1-score provides a harmonic mean for imbalanced risk-level distributions. The AUC further assesses the model's ranking capability across different risk thresholds. This mapping ensures that conventional classification metrics are consistent with the underlying decision-making task. The study also selected the traditional KPCA-TOPSIS method, PCA-TOPSIS and TOPSIS for controlled experiments. The judgment accuracy, AUC value and F1-score are illustrated in Figure 6.

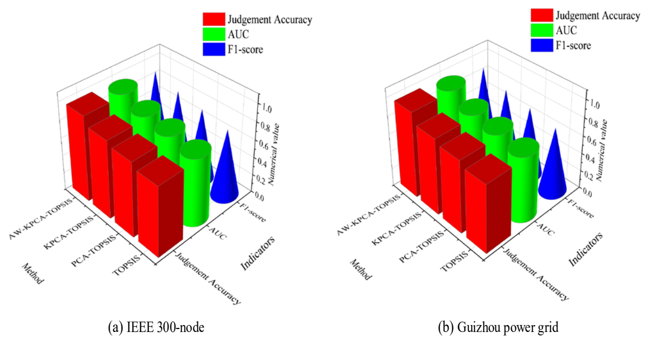

Figure 6. Comparison of comprehensive evaluation results for forced transmission adaptability

In Figure 6, On the IEEE 300-node data set, the judgment accuracy of the AW-KPCA-TOPSIS model reached 95.7%, which was 9.2% higher than that of the traditional KPCA-TOPSIS (86.5%), 13.4% higher than that of the traditional PCA-TOPSIS (82.3%), and 18.9% higher than that of direct TOPSIS (76.8%). The AUC value (0.948) and F1-score (0.941) were better than those of the three traditional methods. On the Guizhou Power Grid Actual Fault Data Set, the proposed model also achieved optimal performance, with a judgment accuracy of 95.3%, and both AUC value (0.942) and F1-score (0.936) were significantly higher. In summary, the proposed AW-KPCA-TOPSIS has a high accuracy and can provide reliable theoretical and algorithmic support for power grid forced transmission decisions.

Finally, the study divided the 259 samples in the IEEE 300-node test set into four groups according to fault types: SG (68), TSC (62), TGS (65), and TPS (64). The confusion matrices of the four methods on each group were calculated separately. The results are shown in Figure 7.

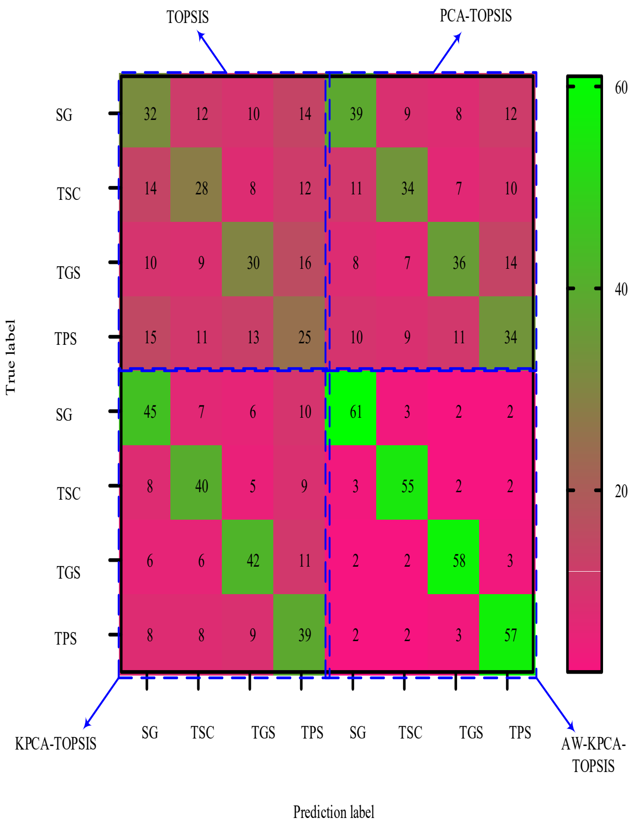

Figure 7. Confusion matrix

In Figure 7, the correct numbers of the proposed model in the SG, TSC, TGS, and TPS reached 61, 55, 58, and 57, respectively, and the total correct number was 231, which was 39.2% higher than that of the traditional KPCA-TOPSIS (total correct number: 166), showing significant advantages. In terms of misclassification distribution, TOPSIS had serious cross-type misclassifications. However, the proposed model controlled the quantity of samples that were misclassified from each fault type to other types within 3, and the misclassification rate was greatly reduced. In summary, the proposed AW-KPCA-TOPSIS is better than the three traditional methods in fault type recognition accuracy and classification stability, verifying the excellent performance of adaptive weighted dimensionality reduction and multi-attribute decision-making fusion in complex fault scenarios.

4. Discussion

To break through the theoretical bottlenecks in the traditional judgment on the adaptability of power grid forced transmission, such as the strong coupling of multi-dimensional influencing factors and the prominent subjectivity of decision-making, a comprehensive judgment model on the adaptability of power grid forced transmission was proposed. In simulation experiments, the proposed method achieved significant performance improvements in multiple dimensions. The training time of AW-KPCA on the IEEE 300-node data set was 7.35 seconds, which was 41.3% lower than that of traditional KPCA (12.54 seconds). The feature extraction accuracy reached 95.3%, which was 15.7% higher than that of traditional KPCA (82.4%). In terms of comprehensive judgment, the AW-KPCA-TOPSIS model had an accuracy of 95.7% on the IEEE 300-node data set, which was 9.2% higher than that of the traditional KPCA-TOPSIS (86.5%). In terms of fault type identification, the total correct number of the proposed model on the four types of faults reached 231, which was 39.2% higher than that of the traditional KPCA-TOPSIS (166). The number of misclassified samples for each fault type was controlled within 3, and the misclassification rate was greatly reduced.

Varbella A [19] proposed a multi-task graph data set construction method for power system power flow, optimal power flow and cascading failure analysis in view of the lack of open and standardized graph neural network training and benchmark data sets in power grid analysis. The proposed method achieved systematic optimization in feature dimensionality reduction efficiency, nonlinear feature retention ability, multi-attribute decision-making accuracy, and classification robustness under complex fault scenarios. Different from the research, this report is to construct a standardized, multi-task graph data set for graph neural networks, which is a construction and benchmarking method at the data resource level. The proposed method is to integrate the multi-dimensional feature matrix, information entropy weighting, AW-KPCA dimensionality reduction and TOPSIS multi-attribute decision-making to form a complete set of force-feeding adaptability judgment algorithm framework. In addition, SU S et al. [20] built an anomaly sensing method using KPCA-OPTICS and quantile regression in view of the lack of professional monitoring of distributed photovoltaic power plants and the difficulty in accurately locating abnormal points. The method had a high detection rate and accuracy and a low false alarm rate in distributed photovoltaic power anomaly detection, and the model had good scalability in actual deployment. The results are similar to the research.

In summary, the AW-KPCA-TOPSIS enhances the accuracy and robustness of the power grid forced transmission adaptability judgment by introducing information entropy adaptive weighting, PSO collaborative optimization weighted kernel dimensionality reduction, and TOPSIS multi-attribute decision-making. The proposed model explicitly incorporates the hybrid energy storage system as the core control object at the methodological level. By expanding the feature dimension and jointly optimizing PSO, it achieves integrated decision-making for energy storage scheduling and grid stability. Although the dataset used for simulation verification does not explicitly contain the measured data of HESS, the model framework itself has the complete modeling capability for energy storage variables, and the information entropy weighting and adaptive dimension reduction mechanism can naturally be extended to any additional feature dimensions. In the future, based on the actual grid data containing HESS, the economicity and robustness of this framework will be further verified.

5. Conclusion

To overcome the limitations of traditional forced transmission assessments, which overlook the active regulation of HESS and the coupling between storage dispatch and grid stability, this paper proposes a collaborative AI optimization and state assessment model centered on HESS. This model incorporates HESS operational state variables based on the multi-dimensional characteristics of the grid, and achieves subjective-objective weighting through information entropy. An adaptive weighted kernel principal component analysis algorithm is proposed, which uses particle swarm optimization to jointly optimize the kernel parameters, feature weights, and energy storage charging and discharging strategies. Furthermore, the TOPSIS multi-attribute decision-making method is integrated to output the optimal energy storage scheduling plan and the risk level of forced power transmission. The core innovations are the explicit integration of HESS dynamics into grid feature modeling, the joint optimization of feature reduction and storage dispatch via PSO-AW-KPCA, and the quantified risk-level output enabled by TOPSIS. Simulation results show that the proposed model can effectively achieve the collaborative optimization of energy storage and the grid, significantly improving the accuracy of forced power transmission decisions after faults and the economic performance of the system operation. However, the research still has shortcomings. The current model depends on IEEE standard system simulation data and Guizhou power grid historical fault data. It does not have sufficient sample coverage under extreme working conditions, and the model's generalization ability in rare scenarios needs to be further verified. Future research can further introduce transfer learning or generative adversarial network technology to expand the extreme scene sample library and optimize the model's adaptability in few-sample scenarios.

Acknowledgments

This research was supported by the National Science and Technology Project on Research and System-Development of Automatic Re-closure Technology for Main-Network Fault Judgment Based on Artificial Intelligence [Project No.: GZKJXM20240254], for which we express our sincere gratitude.

References

[1] B. Yang, R. Zheng, Y. Han, et al., "Recent advances in fault diagnosis techniques for photovoltaic systems: A critical review," Prot. Control Mod. Power Syst., vol. 9, no. 3, pp. 36-59, May 2024, doi: 10.23919/PCMP.2023.000583.

[2] W. Zhuang, J. Fan, M. Xia, et al., "A multi-scale spatial-temporal graph neural network-based method of multienergy load forecasting in integrated energy system," IEEE Trans. Smart Grid, vol. 15, no. 3, pp. 2652-2666, May 2024, doi: 10.1109/TSG.2023.3315750.

[3] F. M. Shakiba, S. M. Azizi, M. Zhou, and A. Abusorrah, "Application of machine learning methods in fault detection and classification of power transmission lines: A survey," Artif. Intell. Rev., vol. 56, no. 7, pp. 5799-5836, Jul. 2023, doi: 10.1007/s10462-022-10296-0.

[4] M. N. Ali, M. Amer, and M. Elsisi, "Reliable IoT paradigm with ensemble machine learning for faults diagnosis of power transformers considering adversarial attacks," IEEE Trans. Instrum. Meas., vol. 72, no. 2, pp. 1-13, Feb. 2023, doi: 10.1109/TIM.2023.3300444.

[5] B. A. Tama, M. Vania, S. Lee, and S. Lim, "Recent advances in the application of deep learning for fault diagnosis of rotating machinery using vibration signals," Artif. Intell. Rev., vol. 56, no. 5, pp. 4667-4709, May 2023, doi: 10.1007/s10462-022-10293-3.

[6] T. Wang, L. Zhang, and X. Wang, "Fault detection for motor drive control system of industrial robots using CNN-LSTM-based observers," CES Trans. Electr. Mach. Syst., vol. 7, no. 2, pp. 144-152, Jun. 2023, doi: 10.30941/CESTEMS.2023.00014.

[7] A. S. Alhanaf, M. Farsadi, and H. H. Balik, "Fault detection and classification in ring power system with DG penetration using hybrid CNN-LSTM," IEEE Access, vol. 12, no. 2, pp. 59953-59975, Feb. 2024, doi: 10.1109/ACCESS.2024.3394166.

[8] J. Hang, X. Shu, S. Ding, et al., "Robust open-circuit fault diagnosis for PMSM drives using wavelet convolutional neural network with small samples of normalized current vector trajectory graph," IEEE Trans. Ind. Electron., vol. 70, no. 8, pp. 7653-7663, Aug. 2023, doi: 10.1109/TIE.2022.3231304.

[9] M. Hajji, Z. Yahyaoui, M. Mansouri, et al., "Fault detection and diagnosis in grid-connected PV systems under irradiance variations," Energy Rep., vol. 9, no. 2, pp. 4005-4017, Mar. 2023, doi: 10.1016/j.egyr.2023.03.033.

[10] M. Kouraichi, M. Mansouri, M. Trabelsi, et al., "Deep learning for fault diagnosis in power transmission lines: Current trends, limitations, and future directions," IEEE Access, vol. 13, pp. 192105-192142, 2025, doi: 10.1109/ACCESS.2025.3628908.

[11] J. Mathebula and N. Mbuli, "Application of TOPSIS in power systems: A review," in 2024 Int. Conf. Electr., Comput. Energy Technol. (ICECET), IEEE, 2024, pp. 1-6, doi: 10.1109/ICECET61485.2024.10698355.

[12] S. Wang, Y. Fu, W. Zhang, C. Fernandez, and F. Blaabjerg, "Review on improved neural network

algorithms for battery state of energy estimation i n smart grids," Renew. Sustain. Energy Rev., vol. 231, p. 116797, May 2026, doi: 10.1016/j.rser.20 26.116797.

[13] S. Wang, H. Gao, P. Takyi-Aninakwa, et al., "Im proved multiple feature-electrochemical thermal co upling modeling of lithium-ion batteries at low-te mperature with real-time coefficient correction," Pr ot. Control Mod. Power Syst., vol. 9, no. 3, pp. 157-173, May 2024, doi: 10.23919/PCMP.2023.000 257.

[14] S. Wang, C. Ma, H. Gao, et al., "Improved hyper parameter Bayesian optimization-bidirectional long short-term memory optimization for high-precision battery state of charge estimation," Energy, vol. 328, p. 136598, Aug. 2025, doi: 10.1016/j.energy. 2025.136598.

[15] S. Aziz, A. Qaiser, U. Kulsoom, et al., "Fault det ection and fault diagnosis in power system using AI: A review," Sir Syed Univ. Res. J. Eng. Tech nol., vol. 14, 10.19781/j.issn.1673-9140.2026.01.01 7. no. 1, pp. 27-32, Jan. 2024, doi: 10.33317/ssurj. 598.

[16] W. Liu, Z. Zhou, K. Cai, et al., "Application of knowledge graph in smart grid fault diagnosis," A ppl. Math. Nonlinear Sci., vol. 8, no. 2, pp. 349- 360, Jul. 2023, doi: 10.2478/amns.2021.2.00258.

[17] J. Liang, K. Zhang, A. Al-Durra, and D. Zhou, " A multi-information fusion algorithm to fault diag nosis of power converter in wind power generatio n systems,"
IEEE Trans. Ind. Inform., vol. 20, no. 2, pp. 1167-117 9, Feb. 2024, doi: 10.1109/TII.2023.3271358.

[18] C. Jiang, H. Xu, W. Jin, et al., "Research on app lication of power Internet of Things technology in leakage fault diagnosis of rural power grid," Ene rgy Rep., vol. 9, no. 2, pp. 847-854, Apr. 2023, doi: 10.1016/j.egyr.2023.04.164.

[19] A. Varbella, K. Amara, B. Gjorgiev, and G.
Sansavini, "PowerGraph: A power grid benchmark data set for graph neural networks," in Adv. Neural In f. Process. Syst., vol. 37, 2024, pp. 110784-11080 4, doi: 10.52202/079017-3517.

[20] S. Su, X. Li, Z. Li, et al., "A distributed photovo ltaic power anomaly perception method based on KPCA-OPTICS clustering," J. Electr. Power Sci. Technol., vol. 41, no. 1, pp. 174-184, Jan. 2026, doi: